

# Measuring the thermal conductivity of the GaN buffer layer in AlGaN/GaN HEMTs: Effect of carbon and iron doping

M.Power<sup>1,\*</sup>, J.W. Pomeroy<sup>1</sup>, Y.Otoki<sup>2</sup>, T.Tanaka<sup>2</sup>, J.Wada<sup>2</sup>, M. Kuzuhara<sup>3</sup>, W.Jantz<sup>4</sup>, A.Souzis<sup>5</sup> and M.Kuball<sup>1</sup>

<sup>1</sup>Center for Device Thermography and Reliability (CDTR), University of Bristol, Bristol BS8 1TL, UK

<sup>2</sup>Hitachi Metals, Ltd., Isagozawa 880, Hitachi City, Ibaraki 319-1418, Japan

<sup>3</sup>Department of Electrical and Electronics Engineering, University of Fukui, Japan

<sup>4</sup>SemiMap Scientific Instruments GmbH, Freiburg, Germany

<sup>5</sup>II-VI Wide Bandgap Group, Pine Brook, NJ 07058, USA

\* Phone: +44 117 928 8750 FAX: +44 117 925 5624 EMAIL: maire.power@bristol.ac.uk

## Introduction and purpose of work

During operation, AlGaIn/GaN high electron mobility transistors (HEMTs) exhibit a temperature rise in the active GaN region of the device which affects reliability and performance. One of the main determining factors of this temperature rise is the thermal conductivity of the GaN active layer which is often assumed to be  $150\text{-}160\text{ Wm}^{-1}\text{K}^{-1}$  [1] in thermal simulations in order to estimate the peak channel temperature rise in the device. However, there is little experimental validation of the actual thermal conductivity ( $\kappa$ ) of transistor epitaxial GaN layers which may be dependent on the dopants used and their concentrations such as, for example, carbon (C) doping [2] for power transistors or iron (Fe) doping [3] for microwave transistors. The temperature gradient within the GaN layer is required to verify the thermal conductivity of this layer and therefore verify the peak channel temperature estimation in reliability studies. This abstract describes a novel technique combining diamond micro-thermometry and micro-Raman thermography to determine the temperature gradient within the carbon-doped (concentration of  $10^{17}\text{cm}^{-3}$ ) GaN layer of an AlGaIn/GaN ungated HEMT. Diamond micro-thermometry and micro-Raman thermography measure the surface temperature and average temperature depth-wise of the GaN layer respectively with the difference in these temperatures related to the temperature gradient. Utilising finite element thermal simulation the thermal conductivity of the GaN layer was determined. This value was used in the thermal modelling of an AlGaIn/GaN HEMT of the same epilayer structure to validate the peak channel temperature estimation of the transistor. The work also aims to discuss the impact of carbon and iron-doping on the thermal properties of AlGaIn/GaN HEMTs.

## Results and Discussion

Ungated and gated AlGaIn/GaN single-finger HEMTs with epilayer structures shown in Fig. 1, grown by metal organic chemical vapour deposition (MOCVD) on  $370\text{ }\mu\text{m}$ -thick vanadium-doped 6H-SiC substrates were studied. Ungated HEMT A and ungated HEMTs B and C were DC-biased at a power of  $1.23\text{W}$  and  $0.98\text{W}$  respectively. HEMT A was

operated with a source-drain bias of  $39.6\text{V}$  and gate voltage of  $0\text{V}$ , giving a power dissipation of  $1.86\text{W}$ .

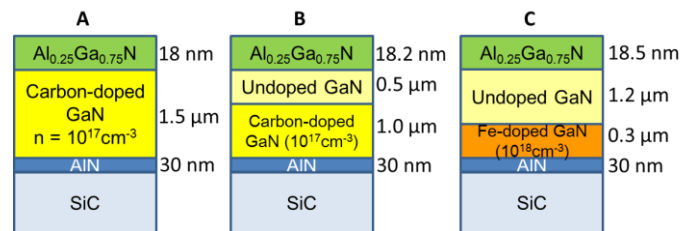
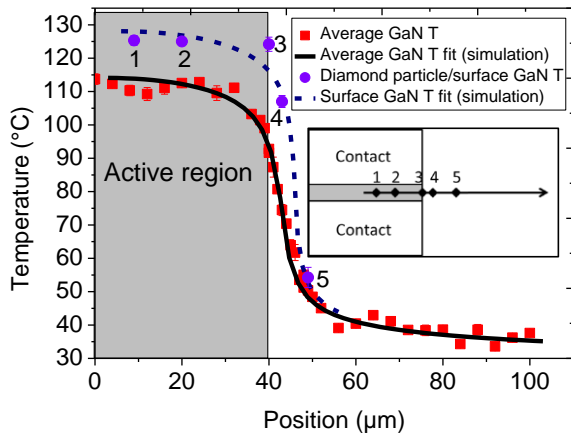


**Fig. 1** Epilayer structures of three (A-C) AlGaIn/GaN HEMTs under investigation where  $n$  is doping concentration.

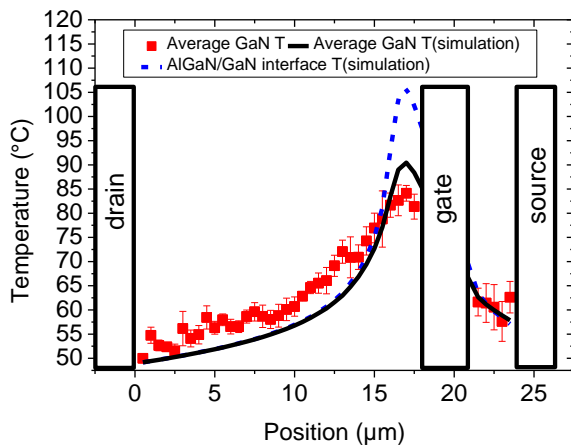
Fig. 2 shows the measured (depth average) GaN temperature profile across ungated HEMT A, from the centre of the device channel to  $60\text{ }\mu\text{m}$  outside the device along with the temperature of four diamond particles (1-5) deposited on the ungated transistor channel area, at positions shown in the inset. Due to thermal equilibrium being reached in these DC measurements the diamond particle temperatures are assumed to be the same as the surface temperature of the GaN layer underneath the particles at the point of contact. Least squares fitting of the thermal simulation to the GaN layer temperature gradient yielded a thermal conductivity of  $185\text{ Wm}^{-1}\text{K}^{-1}$  for the  $1.5\text{ }\mu\text{m}$ -thick carbon-doped GaN layer. Fitting of the simulation to the absolute surface and average GaN temperatures gave a thermal boundary resistance (TBR) of  $2.7 \times 10^{-9}\text{ W}^{-1}\text{m}^2\text{K}$  for the AlN layer.

Fig. 3 shows experimental and simulated (using the previously determined thermal conductivity value of  $185\text{ Wm}^{-1}\text{K}^{-1}$  for the carbon-doped GaN buffer layer and TBR of  $2.7 \times 10^{-9}\text{ W}^{-1}\text{m}^2\text{K}$  for the AlN layer) GaN average temperature profiles from drain to source of HEMT A. It can be seen that the simulated GaN average temperature profile from drain to source contact fits the experimental data quite well within experimental error. The highest temperature is located near the drain edge of the gate contact. This verifies the thermal conductivity of the carbon-doped GaN layer which was extracted by correlating the simulated and experimentally-determined GaN

temperature gradient of the ungated transistor. A simulated temperature profile from drain to source at the AlGaN/GaN interface is also shown. The verified thermal conductivity value gives us confidence in the simulated peak channel temperature at the drain edge of the gate.



**Fig. 2** Experimentally-determined average GaN temperature profile of ungated HEMT A from the centre of the active region to outside this region, surface GaN temperature with diamond particles 1-5 (shown in inset) and best fit of thermal simulation to the experimental data using a thermal conductivity of  $185 \text{ Wm}^{-1}\text{K}^{-1}$  for the GaN layer and a TBR of  $2.7 \times 10^{-9} \text{ W}^{-1}\text{m}^2\text{K}$  for the AlN layer.



**Fig. 3** Experimentally-determined GaN layer average temperature profile and simulated GaN average and AlGaN/GaN interface temperature profiles from drain to source of HEMT A using GaN layer thermal conductivity of  $185 \text{ Wm}^{-1}\text{K}^{-1}$  and a TBR of  $2.7 \times 10^{-9} \text{ W}^{-1}\text{m}^2\text{K}$  for the AlN layer.

Fig. 4 shows the measured (depth average) GaN temperature profile across ungated HEMTs B and C from fig. 1, from the centre of the device channel to  $60 \mu\text{m}$  outside the devices. It can be seen that the temperature rise in the channel of both devices is the same indicating that there is no difference in the effect of carbon and iron-doping on the thermal conductivity of the GaN buffer layer at the doping concentrations used.

Overlaid is a simulated average GaN temperature profile of device B using a thermal conductivity of  $185 \text{ Wm}^{-1}\text{K}^{-1}$  for both the undoped and doped layers. The simulation fits the temperature profile of both devices indicating that the carbon and iron-doping have little or no effect on the thermal conductivity of the GaN layer, for the dopant concentrations considered here.

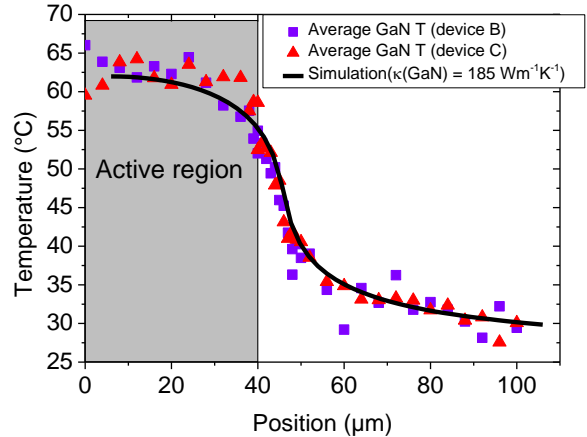


**Fig. 4** Experimentally-determined average GaN temperature profile of ungated HEMTs B and C described in fig. 1 from centre of the active region to outside this region and simulated average GaN temperature profile of device B with  $\kappa(\text{undoped GaN})$  and  $\kappa(\text{carbon-doped GaN})$  as  $185 \text{ Wm}^{-1}\text{K}^{-1}$ .

## Advancement of CS manufacturing

The technique described in this abstract for determining the thermal conductivity of GaN buffer layers in AlGaN/GaN HEMT structures does not require the fabrication of additional test structures such as, for example, a metal contact needed for time-domain thermoreflectance [4]. This is advantageous as it means a standard device wafer can be used. The experimental determination of the thermal conductivity of the GaN buffer layer in the device structure allows for the verification of the peak channel temperature in device thermal modelling which is important in reliability studies. It has also been found that carbon-doping and iron-doping of the GaN buffer layer at concentrations of  $10^{17} \text{ cm}^{-3}$  and  $10^{18} \text{ cm}^{-3}$  respectively have no significant effect on the thermal conductivity.

## References

- 1) J. W. Pomeroy, M. Kuball, D. J. Wallis, A. M. Keir, K. P. Hilton, R. S. Balmer, M. J. Uren, T. Martin and P. J. Heard, *Appl. Phys. Lett.* **87**, 103508 (2005)
- 2) E. Bahat-Treidel, F. Brunner, O. Hilt, E. Cho, J. Würfl and G. Tränkle, *IEEE Trans. Electron Devices* **57**, 3050 (2010).
- 3) M. J. Uren, D. G. Hayes, R. S. Balmer, D. J. Wallis, K. P. Hilton, J. O. Maclean, T. Martin, C. Roff, P. McGovern, J. Benedikt and P. J. Tasker, *Eur Microw Integrat.* **65** (2006)
- 4) J. Cho, Y. Li, W. E. Hoke, D. H. Altman, M. Asheghi and K. E. Goodson, *Phys. Rev. B*, **89**, 115301 (2014).